available at www.sciencedirect.com

ScienceDirect

journal homepage: www.elsevier.com/locate/chnjc

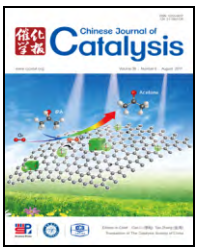

Article

Synthesis and characterization of a Pd(0) Schiff base complex anchored on magnetic nanoporous MCM-41 as a novel and recyclable catalyst for the Suzuki and Heck reactions under green conditions

Mohsen Nikoorazm [a,*], Farshid Ghorbani [b], Arash Ghorbani-Choghamarani [a], Zahra Erfani [a]

[a] *Department of Chemistry, Faculty of Science, Ilam University, P. O. Box69315516, Ilam, Iran*

[b] *Department of Environment, Faculty of Natural Resource, University of Kurdistan, Sanandaj 66177-15177, Iran*

ARTICLE INFO

Article history:
Received 7 April 2017
Accepted 16 May 2017
Published 5 August 2017

Keywords:
MCM-41
Magnetic nanoparticles
Suzuki reaction
Heck reaction
Polyethylene glycol (PEG)
Palladium

ABSTRACT

A Pd Schiff base complex was immobilized onto the surface of magnetic MCM-41 (Fe_3O_4@MCM-41@Pd(0)-P2C) as a novel, eco-friendly, and recyclable heterogeneous nanocatalyst and fully characterized by FT-IR, VSM, EDS, transmission electron microscopy, scanning electron microscopy, thermogravimetric analyses, ICP-OES, and X-ray powder diffraction analysis. The Fe_3O_4@MCM-41@Pd(0)-P2C was investigated as a catalyst for the one-pot Suzuki and Heck reactions in PEG as a green solvent to provide the target products in excellent yields. The main advantages of using this catalyst include a short reaction time, green reaction conditions, a simple experimental procedure, non-use of hazardous organic solvents, low loading of the catalyst, and the ability to use various substrates. More importantly, the catalyst could be easily separated from the reaction mixture with the assistance of an external magnet and could be recovered and reused several times without significant loss of stability and activity.

1. Introduction

Molecular sieves and mesoporous materials with regular geometries have attracted much attention owing to their remarkable characteristics such as high surface area, high efficiency, large pore volume, and recyclability compared with nonporous objects [1–4]. Mobil composition of matter No. 41 (MCM-41) as a member of a family of mesoporous molecular sieves, which was reported by Beck et al. [5], consists of mesoporous-structured SiO_2 formed by a hexagonal array of unidirectional pore structures [6,7]. These materials possess unique structural features such as high surface area [8], very narrow pore size distribution [9], and excellent thermal [10], chemical, and mechanical stability [11], which has opened up new possibilities for the design of novel heterogeneous catalysts. Magnetic nanoparticles (MNPs) are an important class of compounds that have received significant attention because of the broad spectrum of biological and medical applications such as drug delivery, biomolecular sensors, magnetic resonance imaging, bioseparation, and magneto-thermal therapy as well as in catalysis, environmental depollution, and in vitro/in vivo applications [12,13]. MNPs have been widely used in catalytic reactions as heterogeneous catalysts. The advantages of using magnetic nanoparticles as heterogeneous catalysts include ease of recovery from the reaction mixture using an external magnet [14], their large surface area ratio, and ease of preparation.

* Corresponding author. Tel/Fax: +98-843-2227022; E-mail: e_nikoorazm@yahoo.com
DOI: 10.1016/S1872-2067(17)62865-1 | http://www.sciencedirect.com/science/journal/18722067 | Chin. J. Catal., Vol. 38, No. 8, August 2017

MNPs have been used as a core for the support of catalyst used in organic transformations owing to coupling with organic ligands and inorganic compounds [10]. The design and synthesis of efficient and recoverable catalysts has become an important environmental and economical consideration for industrial applications [15]. One strategy in this area has focused on the consolidation of functionalized mesoporous silica materials with magnetic nanoparticles to form a porous magnetic nanocomposite. These types of magnetic nanocomposites have the properties and advantages of both mesoporous silica and magnetic nanoparticles [16] and have been used for magnetic storage and recording, catalytic applications, sensors, environmental, and biomedical applications [12]. Reactions leading to the formation of C–C bonds catalyzed by palladium complexes, such as Suzuki and Heck coupling reactions, have become powerful methods in modern synthetic organic chemistry for the preparation of natural products, ultraviolet (UV) screens, pharmaceuticals, biologically active compounds, hydrocarbons, polymers, liquid crystal materials, and advanced materials [17–19]. Homogeneous palladium catalysts have been extensively studied in synthetic organic chemistry because of their high selectivity and catalytic activity [20]. Homogeneous catalytic reactions have many disadvantages such as poor reusability and separation of the catalysts from the reaction mixture. These disadvantages can be minimized by immobilizing homogenous catalysts on polymeric organic or inorganic supports [21,22]. In this study, Pd complexes were anchored to porous magnetic nanocomposites as a catalyst support and employed as excellent and reusable heterogeneous organometallic nanocatalysts for C–C Suzuki and Heck coupling reactions. The main advantage of this catalytic system was the use of PEG as a green solvent to provide the target products in excellent yields in short reaction times. The nanoparticles could be easily isolated from the product solution by using an external magnet after completing the reactions.

2. Experimental

2.1. Materials and characterization

The cetyltrimethylammonium bromide (CTAB; 98%), tetraethyl orthosilicate (TEOS), 3-aminopropyltriethoxysilane (3-APTES), $FeCl_3{\cdot}6H_2O$, $FeCl_2{\cdot}4H_2O$, palladium acetate, phenylboronic acid, and solvents were purchased from Aldrich, Merck, and Flucka and were used as received without further purification. The nanostructures were identified using a Holland Philips X'pert X-ray powder diffraction (XRD) diffractometer at a scanning speed of 2°/min from 1° to 80°. Fourier transform infrared (FT-IR) spectra were recorded with KBr pellets utilizing a VRTEX 70 model Bruker FT-IR spectrometer. Thermogravimetric analyses (TGA) of the samples were carried out between 30 and 800 °C using a Shimadzu DTG-60 automatic thermal analyzer. The particle size and morphology were examined by scanning electron microscopy (SEM) using a FESEM-TESCAN MIRA3, as well by high-resolution transmission electron microscopy (TEM) with a JEOL JEM-2100F, 200kV transmission electron microscope. The VSM measurements were performed using a vibrating sample magnetometer (VSM) MDKFD. Magnetization measurements were carried out using an external field of up to 15 kOe at several temperatures. The Pd content was measured using inductively coupled plasma-optical emission spectrometry (ICP-OES).

2.2. Preparation of Fe_3O_4@MCM-41

Magnetic Fe_3O_4 nanoparticles were prepared as follows. A mixture of $FeCl_3{\cdot}6H_2O$ (2 g) and $FeCl_2{\cdot}4H_2O$ (0.8 g) were dissolved in 10 mL of deionized water under a N_2 atmosphere. The mixture was added to 100 mL of 1.0 mol/L NH_3 solution containing 0.4 g of CTAB under sonication and a N_2 atmosphere. After 30 min, the reaction was completed, the Fe_3O_4 nanoparticles were isolated by magnetic decantation and dried at 80 ˚C under vacuum [23]. The Fe_3O_4@MCM-41 was prepared by the following method. First, Fe_3O_4 nanoparticles (0.05 g) were dispersed in ethanol (20.0 mL) for 30 min by using ultrasonication. Then, the suspension was centrifuged and the solid was re-dispersed in a mixture of deionized water (10 mL), ethanol (20 mL), and NH_3 (0.5 mL). The system was kept under vigorous mechanical stirring for 30 min, and then TEOS (0.03 g) was added dropwise. The mixture was stirred at room temperature for 6 h. The coated nanoparticles (Fe_3O_4@$n$$SiO_2$) were separated by decantation with the aid of a magnet and washed with ethanol and water several times. In the second step, the coated Fe_3O_4@$n$$SiO_2$ nanoparticles were dispersed in a mixture of deionized water (40 mL), ethanol (30 mL), NH_3 (0.6 mL), and CTAB (0.15 g). After stirring at room temperature for 30 min, 0.4 g of TEOS (as a silica source) was added slowly to the solution and stirring was continued for another 6 h. After completion of the reaction, the solid products were collected by magnetic separation, washed with plenty of ethanol/deionized water, and subsequently dried in a vacuum oven at 80 °C for 12 h. To remove the CTAB template, ethanol (100 mL) and 5 mL of 2 mol/L HCl were added to 0.1 g of the produced nanocomposite, then the mixture was stirred at room temperature for 48 h. The solid products were collected by magnetic separation and subsequently dried in a vacuum oven at 80 °C for 24 h. The resulting solid was referred to as Fe_3O_4@MCM-41.

2.3. Preparation of 3-APTES functionalized Mag-mesoporous silica (Fe_3O_4@MCM-41-NH_2)

To a suspension of Fe_3O_4@MCM-41(4.8 g) in n-hexane, 4.8 g of 3-aminopropyltriethoxysilane (3-APTES) was added slowly under a N_2 atmosphere at 80 °C and refluxed for 24 h. The separated solid Fe_3O_4@MCM-41-$(SiCH_2CH_2CH_2NH_2)_x$ was collected by magnetic separation, washed with n-hexane, and dried under vacuum.

2.4. Preparation of heterogeneous Pd Schiff base complex grafted in Mag-mesoporous silica (Fe_3O_4@MCM-41@Pd(0)-P2C)

For the preparation of Fe_3O_4@MCM-41@P2C, a solution of 0.5 g Fe_3O_4@MCM-41@nPr-NH_2 and pyrrole-2-carbaldehyde (1.2 mmol) in ethanol was refluxed under a N_2 atmosphere for

3 h. The resulting solid was washed with ethanol, collected by magnetic separation and dried under vacuum and designated as Fe_3O_4@MCM-41@P2C. Ultimately, the Fe_3O_4@MCM-41@Pd(0)-P2C was prepared by refluxing a solution of $Pd(OAc)_2$ (0.63 mmol, 0.168 g) with 0.250 g Fe_3O_4@MCM-41@P2C in ethanol (20 mL) for 20 h. Finally, Pd(II) was reduced with $NaBH_4$ (0.057 mmol, 0.022 g) under the same conditions for another 2 h. The resulting black solid impregnated with the metal complex was separated by a magnet and washed with ethanol to give the Pd(0) complex. The detailed preparation route for Fe_3O_4@MCM-41@Pd(0)-P2C is shown in Scheme 1.

2.5. General procedure for the Suzuki coupling reaction

A mixture of an aryl halide (1 mmol), phenylboronic acid (1 mmol), K_2CO_3 (3 mmol), and Fe_3O_4@MCM-41@Pd(0)-P2C (0.004 g, 0.66 mol%) was added to a reaction vessel. The resulting mixture was stirred in PEG-400 at 60 °C and the progress of the reaction was monitored by thin-layer chromatography (TLC). After completion of the reaction, the catalyst was separated using an external magnet and washed with ethyl acetate. The reaction mixture was extracted with ethyl acetate and water, and the organic layer was dried over anhydrous Na_2SO_4 (1.5 g). The solvent was evaporated and pure products were obtained in good to excellent yields.

2.6. General procedure for the Heck reaction

A mixture of an aryl halide (1 mmol), an alkene (1.2 mmol), K_2CO_3 (3 mmol), and Fe_3O_4@MCM-41@Pd(0)-P2C (0.006 g, 0.99 mol%) was stirred in PEG-400 at 120 °C and the progress of the reaction was monitored by TLC. After completion of the reaction, the mixture was cooled to room temperature. The catalyst was separated by an external magnet and washed with diethyl ether. The reaction mixture was extracted with water and diethyl ether. The organic layer was dried over Na_2SO_4 (1.5 g) and the solvent was evaporated to obtain the pure products in good to excellent yields.

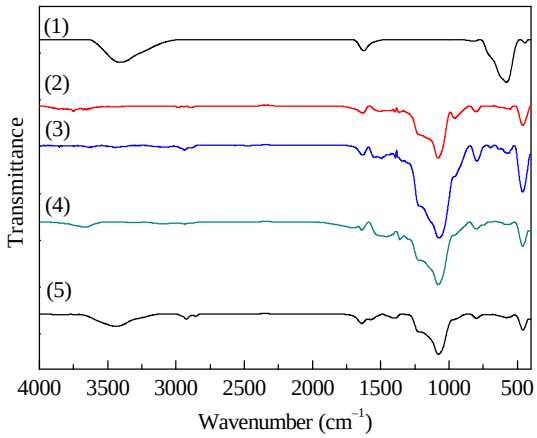

Fig. 1. FT-IR spectra of Fe_3O_4 (1), Fe_3O_4@MCM-41 (2), Fe_3O_4@MCM-41@nPr-NH_2 (3), Fe_3O_4@MCM-41@P2C (4), and Fe_3O_4@MCM-41@Pd(0)-P2C (5).

3. Results and discussion

3.1. Characterization of Fe_3O_4@MCM-41@Pd(0)-P2C

The structure of the Palladium Schiff base complex anchored onto the surface of magnetic MCM-41 (Fe_3O_4@MCM-41@Pd(0)-P2C) was studied and fully characterized by FT-IR, VSM, EDS, TEM, SEM, XRD, and TGA analysis. Fig. 1 shows the FT-IR spectra of the synthesized Fe_3O_4, Fe_3O_4@MCM-41, Fe_3O_4@MCM-41-NH_2, Fe_3O_4@MCM-41@P2C, and Fe_3O_4@MCM-41@Pd(0)-P2C. The FT-IR spectrum of the Fe_3O_4 nanoparticles (Fig. 1(1)) displayed strong absorptions at

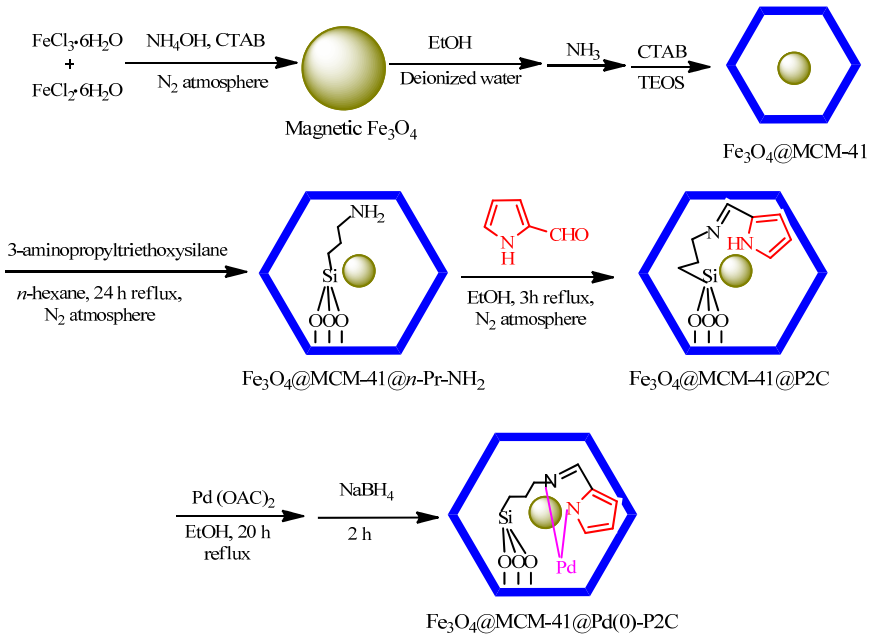

Scheme 1. Synthesis of Fe_3O_4@MCM-41@Pd(0)-P2C.

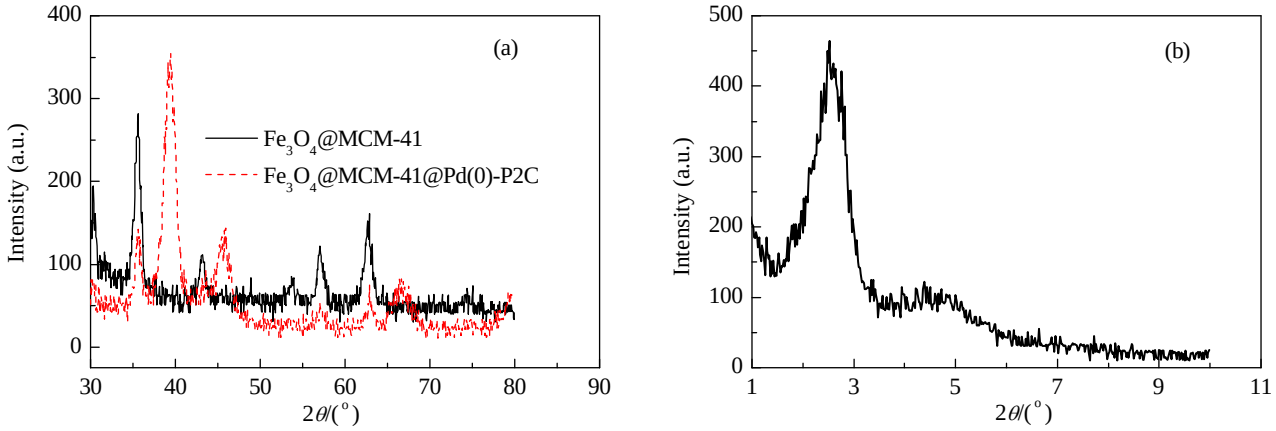

Fig. 2. (a) Wide angle XRD patterns of Fe_3O_4@MCM-41 and Fe_3O_4@MCM-41@Pd(0)-P2C; (b) Small angle XRD pattern of Fe_3O_4@MCM-41.

579 cm^{-1} and 3000–3500 cm^{-1}, which were assigned to the Fe–O and O–H stretching vibrations [22]. The FT-IR spectrum of the Fe_3O_4@MCM-41 sample (Fig. 1(2)) displayed peaks at 460, 958, and 1081 cm^{-1}, which corresponded to bending, symmetric, and asymmetric stretching of the Si–O–Si vibrations, respectively [25]. The presence of the peak at 1550 cm^{-1}, mainly from NH_2 symmetric bending vibrations, indicated successful attachment of an organic amine onto the Fe_3O_4@MCM-41 surface. The broad band at 3443 cm^{-1} was assigned to the hydrogen bonding between the silanol groups and adsorbed water, and the band at approximately 2939 cm^{-1} was associated with the CH_2 vibrations corresponding to C–H stretching (Fig. 1 (3)). The Fe_3O_4@MCM-41@P2C exhibited a ν(C=N) stretch at 1637 cm^{-1}, which shifted to 1629 cm^{-1} in the FT-IR spectrum of Fe_3O_4@MCM-41@Pd(0)-P2C, indicating the formation of Pd-ligand bonds [2].

The crystalline structures of the catalyst were analyzed by XRD. The wide angle XRD of the Fe_3O_4@MCM-41 and Fe_3O_4@MCM-41@Pd(0)-P2C samples are shown in Fig. 2(a). The characteristic peaks at 2θ = 30.0°, 35.4°, 43.3°, 54.5°, 57.0°, and 62.8° assigned to magnetite were observed, which is consistent with the standard Fe_3O_4 XRD spectrum and demonstrated that the catalyst had been successfully synthesized without damaging the crystal structure of Fe_3O_4 [25]. Furthermore, the XRD pattern of Fe_3O_4@MCM-41@Pd(0)-P2C contained a series of peaks (39.4°, 45.9°, and 66.9°) which were indexed to Pd camouflaged on the surface of Fe_3O_4@MCM-41 [8]. The comparison study of the XRD patterns of Fe_3O_4@MCM-41 and Fe_3O_4@MCM-41@Pd(0)-P2C showed that after grafting of Pd through the formation of a complex with Fe_3O_4@MCM-41, reflections with weaker intensities were observed. As seen from the small angle XRD patterns in Fig. 2(b), The XRD pattern of Fe_3O_4@MCM-41 showed the presence of three reflection peaks corresponding to d_{100}, d_{110}, and d_{200} planes at 2θ = 2.36°, 3.94°, and 4.38°, respectively, confirming the presence of the ordered hexagonal mesoporous structure of MCM-41 [23].

Fig. 3 are the SEM images of Fe_3O_4@MCM-41 and Fe_3O_4@MCM-41@Pd(0)-P2C. The Fe_3O_4@MCM-41 and Fe_3O_4@MCM-41@Pd(0)-P2C materials were composed of nearly spherical agglomerations composed of regular uniform nanoparticles.

The energy dispersive spectrum (EDS) indicated the presence of Pd, Fe, Si, O, N, and C species in the catalyst (Fig. 4).

TEM images of the Fe_3O_4@MCM-41@Pd(0)-P2C are shown in Fig. 5. The HRTEM micrograph demonstrated the ordered mesostructures with uniform pore dimension and hexagonal symmetry and agglomeration of many ultrafine spherical-like particles that displayed dark magnetite cores surrounded by a shell.

The magnetic properties of Fe_3O_4@MCM-41 and Fe_3O_4@MCM-41@Pd(0)-P2C were investigated using VSM at

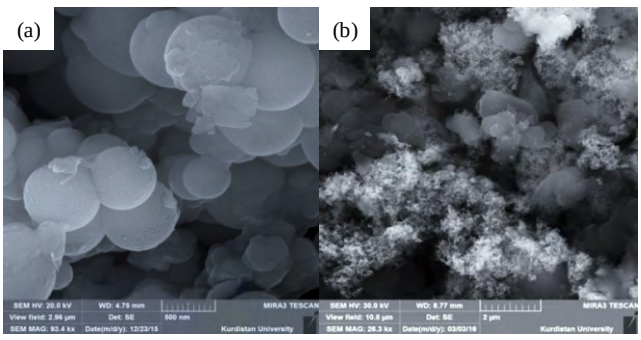

Fig. 3. SEM images of Fe_3O_4@MCM-41 (a) and Fe_3O_4@MCM-41@Pd(0)-P2C (b).

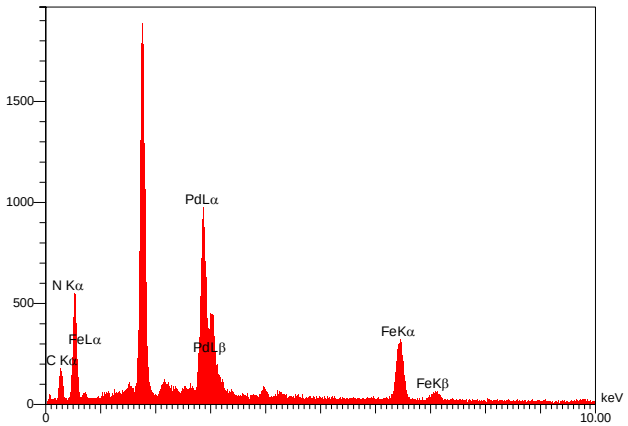

Fig. 4. EDS spectrum of Fe_3O_4@MCM-41@Pd(0)-P2C.

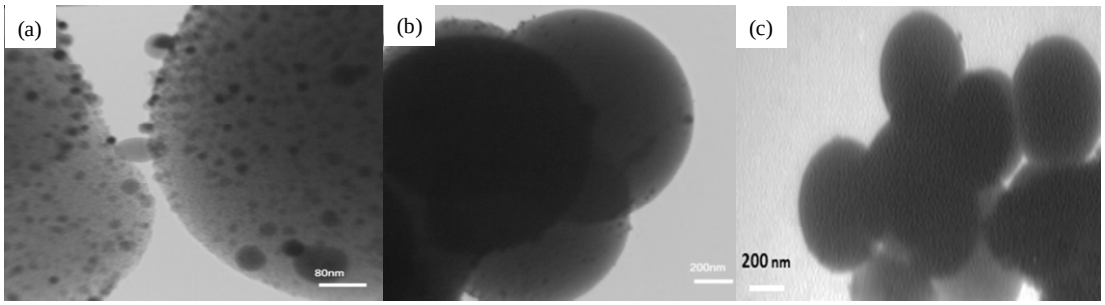

Fig. 5. HRTEM images of Fe_3O_4@MCM-41@Pd(0)-P2C. (a) 80 nm; (b, c) 200 nm.

room temperature (Fig. 6). VSM measurements of the Fe_3O_4@MCM-41 nanoparticles showed that the saturation magnetization (M_s) of Fe_3O_4@MCM-41@Pd(0)-P2C was 9.42 emu/g (Fig. 6(2)), which is lower than the M_s of Fe_3O_4@MCM-41 (13.02 emu/g) (Fig. 6(1)). Based on these results, the successful grafting of organic layers containing a palladium complex on Fe_3O_4@MCM-41 was verified [26].

The thermogravimetric analysis (TGA) curves of Fe_3O_4@MCM-41and Fe_3O_4@MCM-41@Pd(0)-P2C are shown in Fig. 7. The TGA of the synthesized Fe_3O_4@MCM-41 showed a 3% weight loss in one step at a temperature below 100 °C owing to the desorption of water. The Fe_3O_4@MCM-41@Pd(0)-P2C sample showed a mass loss of approximately 2% below 125 °C owing to the removal of physically adsorbed water and solvent inside the pore channels. The other weight losses was in the region of 200–550 °C (approximately 22%), which was mainly related to the decomposition of the organically modified moieties on Fe_3O_4@MCM-41@Pd(0)-P2C [27]; and above 600 °C (about 6%) as a result of the condensation of the silanol groups.

Finally, the exact amount of Pd in the nanostructured catalyst was determined by ICP-OES. The amount of Pd in the immobilized catalyst on Fe_3O_4@MCM-41 was found to be 1.65 mmol/g.

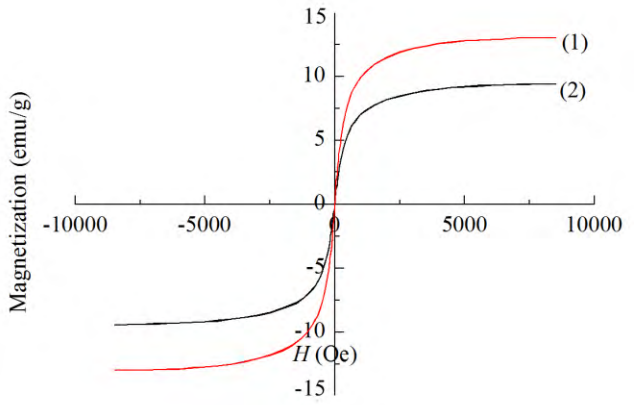

Fig. 6. Magnetic curves of Fe_3O_4@MCM-41 (1) and Fe_3O_4@MCM-41@Pd(0)-P2C (2).

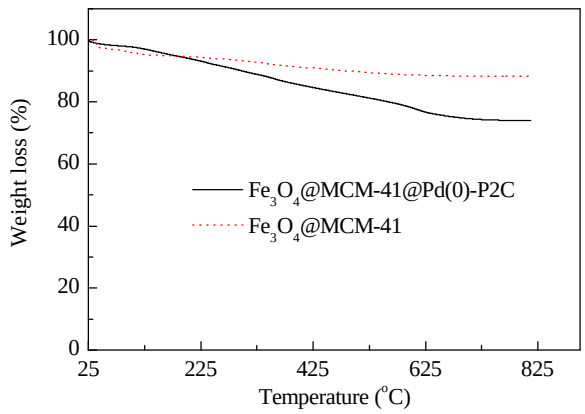

Fig. 7. TGA thermograms of Fe_3O_4@MCM-41 and Fe_3O_4@MCM-41@Pd(0)-P2C.

3.2. Evaluation of the catalytic activity of Fe_3O_4@MCM-41@Pd(0)-P2C in Suzuki-Miyaura and Mizoroki-Heck reactions

After full characterization of the Fe_3O_4@MCM-41@Pd(0)-P2C structure, the catalytic activity of this magnetic mesoporous compound was examined for C–C coupling reactions, namely Suzuki and Heck reactions. To optimize the reaction conditions, the Suzuki coupling reaction of iodobenzene (1 mmol) with phenyl boronic acid (1 mmol) was examined using different amounts of catalyst and solvent at a temperature range of 25–60 °C (Table 1). When the reaction was carried out

Table 1
Optimization of the Suzuki reaction between iodobenzene and phenyl boronic acid under different conditions.

Entry	*T* (°C)	Solvent	Base	Catalyst amount (mg)	Time (min)	Yield* (%)
1	60	PEG-400	K_2CO_3	None	360	Trace
2	60	PEG-400	K_2CO_3	5	20	94
3	60	PEG-400	K_2CO_3	4	20	94
4	60	PEG-400	K_2CO_3	3	20	85
5	60	1,4-dioxane	K_2CO_3	4	20	15
6	60	H_2O	K_2CO_3	4	20	Trace
7	60	DMF	K_2CO_3	4	20	90
8	60	EtOH	K_2CO_3	4	20	85
9	60	PEG-400	Et_3N	4	20	92
10	60	PEG-400	$NaHCO_3$	4	20	86
11	60	PEG-400	Na_2CO_3	4	20	90
12	60	PEG-400	KOH	4	20	Trace
13	50	PEG-400	K_2CO_3	4	20	92
14	40	PEG-400	K_2CO_3	4	20	66
15	25	PEG-400	K_2CO_3	4	20	20

Reaction conditions: iodobenzene (1 mmol), phenyl boronic acid (1 mmol), base (3 mmol), Fe_3O_4@MCM-41@Pd(0)-P2C (4 mg), and PEG-400 (2 mL).
* Isolated yield.

Table 2
Results of the Suzuki reaction catalyzed by Fe_3O_4@MCM-41@Pd(0)-P2C.

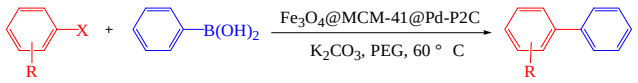

X= I, Br, Cl

Entry	Aryl halide	Time (min)	Yield * (%)	m.p. (°C) Found	m.p. (°C) Reported [Ref.]
1		20	94	64–67	67–68 [28]
2	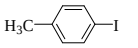	40	96	44–46	44–46 [29]
3		35	98	Oil	Oil [28]
4	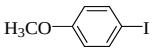	55	91	83–85	84–85 [28]
5	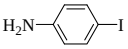	65	88	53–54	50–53 [30]
6		40	93	67–68	67–68 [28]
7	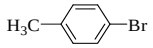	35	94	42–44	44–47 [28]
8	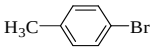	50	90	80–83	84–85 [28]
9	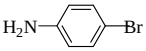	70	90	51–53	50–53 [30]
10	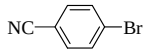	40	93	79–81	82–83 [28]
11	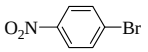	50	92	112–114	112–114 [29]
12	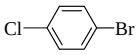	50	94	69–71	70–71 [28]
13	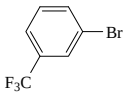	30	93	Oil	Oil [31]
14 [b]		80	94	64–66	67–68 [28]
15 [b]	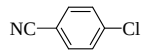	200	90	81–83	82–83 [28]
16 [b]	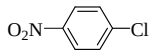	240	92	111–112	112–114 [29]

Reaction conditions: various aryl halides (1 mmol), phenyl boronic acid (1 mmol), K_2CO_3 (3 mmol), 60 °C.
* Isolated yield.
[b] Conditions were as follows: Fe_3O_4@MCM-41@Pd(0)-P2C (6 mg) at 100 °C.

in the absence of catalyst, the reaction was slow and resulted in no product, even after 6 h (Table 1, entry 1). The best result was obtained when the reaction was carried out in presence of 4 mg of catalyst in PEG-400 at 60 °C (Table 1, entry 3). In the next step, we studied the influence of the solvents PEG-400, EtOH, DMF, 1,4-dioxane, and H_2O, at 60 °C (Table 1, entries 3, 5–8). The best results were obtained when PEG-400 was used. We then investigated the effects of the base on the reaction in the PEG solvent at 60 °C. Different bases including $(Et)_3N$, $NaHCO_3$, Na_2CO_3, KOH, and K_2CO_3 were studied (Table 1, entries 3, 9–12). A high yield and shorter reaction time were obtained when K_2CO_3 was employed as base. Therefore, we chose K_2CO_3 as the base in all of the subsequent coupling reactions. We also studied the effect of temperature (Table 1, entries 3, 13–15). The optimum results were obtained at 60 °C.

Table 3
Optimization of the Heck reaction between iodobenzene and *n*-butyl acrylate under different conditions.

Entry	Temperature (°C)	Solvent	Base	Catalyst (mg)	Time (min)	Yield * (%)
1	120	PEG-400	K_2CO_3	None	1440	Trace
2	120	PEG-400	K_2CO_3	3	25	62
3	120	PEG-400	K_2CO_3	4	25	85
4	120	PEG-400	K_2CO_3	6	25	96
5	120	PEG-400	Et_3N	6	25	90
6	120	PEG-400	$NaHCO_3$	6	25	75
7	120	PEG-400	Na_2CO_3	6	25	88
8	120	PEG-400	KOH	6	25	35
9	120	H_2O	K_2CO_3	6	25	—
10	120	DMF	K_2CO_3	6	25	83
11	120	EtOH	K_2CO_3	6	25	78
12	110	PEG-400	K_2CO_3	6	25	87
13	100	PEG-400	K_2CO_3	6	25	68
14	80	PEG-400	K_2CO_3	6	25	54

Reaction conditions: Ar-X (1 mmol), *n*-butyl acrylate (1.2 mmol), base (3 mmol), Fe_3O_4@MCM-41@Pd(0)-P2C (6 mg), and PEG-400 (2 mL).
* Isolated yield.

To demonstrate the efficiency and the scope of Fe_3O_4@MCM-41@Pd-P2C as a catalyst, various aryl halides were reacted with phenyl boronic acid under the optimal reaction conditions to produce the corresponding biphenyls in excellent yields and short reaction times (Table 2). As shown in Table 2, the reaction with chlorobenzene was slower than of iodobenzene or bromobenzene and required a much higher temperature and more Fe_3O_4@MCM-41@Pd(0)-P2C catalyst (6 mg, 0.99 mol%) (Table 2, entries 14–16). The aryl halides containing electron-donating and electron-withdrawing functional groups were converted to the corresponding biphenyls in short reaction times with good yield. As shown in Table 2, for the aryl iodides containing electron-donating functional groups, such as Me and OMe, the reaction was completed after shorter reaction times compared with those containing electron-withdrawing substituents.

To extend the catalytic applications of the Fe_3O_4@MCM-41@Pd(0)-P2C catalyst, we investigated its ability to catalyze the Heck C–C coupling reaction. The reaction of aryl halides with two types of vinylic substrates (*n*-butyl acrylate and acrylonitrile) were employed as the model reaction. The effect of the amount of catalyst, solvent (DMF, 1,4-dioxane, H_2O, EtOH, or PEG), temperature (room temperature to 120 °C), and the nature of the base (Et_3N, K_2CO_3, KOH, $NaHCO_3$, or Na_2CO_3) on the outcome of the coupling of iodobenzene with *n*-butyl acrylate or acrylonitrile was examined. A summary of the results is shown in Table 3. The reaction did not occur in the absence of Fe_3O_4@MCM-41@Pd(0)-P2C (Table 3, entry 1). Among the different amount of catalyst tested, 6 mg (0.99 mol%) was found to be the most effective amount because it gave the highest product yield. Among the different solvents, the best yields were obtained with PEG-400 using 0.006 g (0.99 mol%) of Fe_3O_4@MCM-41@Pd(0)-P2C (Table 3, entry 4). The reaction was significantly affected by the nature of the base; the best result was obtained using K_2CO_3. The coupling reaction

Table 4
Results of the Heck reaction catalyzed by Fe_3O_4@MCM-41@Pd(0)-P2C.

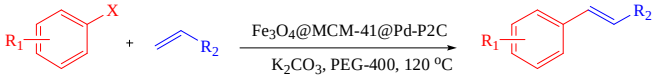

X=Br, Cl, I **R_2**= COOBU, CN

Entry	Aryl halide	Alkene	Time (min)	Yield* (%)	m.p. (°C)	
					Found	Reported [Ref.]
1		Butyl acrylate	25	96	Oil	Oil [32]
2	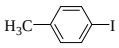	Butyl acrylate	35	94	Oil	Oil [32]
3		Butyl acrylate	85	88	Oil	Oil [32]
4	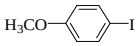	Butyl acrylate	40	90	Oil	Oil [32]
5		Butyl acrylate	80	92	Oil	Oil [32]
6		Butyl acrylate	90	86	Oil	Oil [32]
7	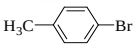	Butyl acrylate	90	80	Oil	Oil [32]
8	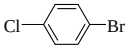	Butyl acrylate	120	92	Oil	Oil [33]
9	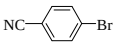	Butyl acrylate	80	91	40–43	40–43 [34]
10		Butyl acrylate	360	87	Oil	Oil [32]
11		Acrylonitrile	65	94	Oil	Oil [35]
12	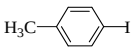	Acrylonitrile	100	93	70–73	72–73 [36]
13		Acrylonitrile	180	95	Oil	Oil [35]
14	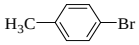	Acrylonitrile	190	92	70–73	72–73 [36]

*Isolated yield.

yields were susceptible to temperature changes (Table 3, entries 4, 11–14). The highest product yield was achieved at 120 °C.

After optimization of the reaction conditions, we examined the catalytic activity of Fe_3O_4@MCM-41@Pd(0)-P2C for other substrates (Table 4). The optimized reaction conditions were applied to a wide range of aryl halides using *n*-butyl acrylate or acrylonitrile. The aryl bromides and aryl iodides required a shorter reaction time compared with the corresponding aryl chloride (Table 4, entry 10).

To compare the catalytic properties of Fe_3O_4@MCM-41@Pd(0)-P2C with those of other catalysts reported in the literature, we investigated the results of the Suzuki-Miyaura reaction between iodobenzene and phenylboronic acid (Table 5) and the Heck-Mizoroki cross-coupling reactions between iodobenzene and butyl acrylate (Table 6) in the presence of various catalysts with respect to the temperature, the yield of the products, solvent, and reaction time. As shown in Tables 5 and 6, in this work, C–C bond forming through the Suzuki and Heck reaction was carried out in PEG-400 with short reaction times and in good to excellent yields. The new catalyst is also non-toxic, stable, cheap and easy to separate. The recoverability and recyclability of this catalyst was faster and easier than that of the other reported catalysts.

Table 5
Comparison of the effect of catalyst with other catalysts for the Suzuki-Miyaura reaction between iodobenzene and phenylboronic acid.

Entry	Catalyst	Conditions	Time (h)	Yield (%)	Ref.
1	Pd-imino-Py-γ-Fe_2O_3	Et_3N, DMF, 100 °C	0.5	95	[35]
2	γ-Fe_2O_3-acetamidine-Pd	Et_3N, DMF, 100 °C	0.5	96	[36]
3	Pd-Py-MCM-41	Na_2CO_3, PEG, 80 °C	2	97	[37]
4	LDH–Pd(0)	K_2CO_3, 1,4-dioxane-H_2O, 80 °C	10	96	[38]
5	MCM-41-S-Pd(0)	K_2CO_3, DMF-H_2O, 80 °C	6	98	[39]
6	Pd-BIP-γ-Fe_2O_3@SiO_2	Et_3N, DMF, 100 °C	1	98	[40]
7	Fe_3O_4-Bpy-Pd(OAc)$_2$	K_2CO_3, Toluene, 80 °C	6	99	[41]
8	Fe_3O_4@SiO_2@mSiO_2-Pd (II)	K_2CO_3, EtOH, 80 °C	3	98	[42]
9	Pd(II)-NHC complex	Cs_2CO_3, DMF, 100 °C	24	99	[43]
10	Fe_3O_4@MCM-41@Pd(0)-P2C	K_2CO_3, PEG, 60 °C	20 min	96	this work

Table 6
Comparison of the effect of catalyst with other catalysts for Heck-Mizoroki cross-coupling reactions from iodobenzene with butyl acrylate.

Entry	Catalyst	Conditions	Time (h)	Yield (%)	Ref.
1	Fe_3O_4@SiO_2/Schiff base/Pd(II)	K_2CO_3, DMF, 110 °C	0.75	97	[44]
2	Pd-NPs	Et_3N, IL, 100 °C	3	87	[45]
3	Pd/Fe_3O_4	K_2CO_3, NMP, 130 °C	5	99	[46]
4	Pd/6c complex	K_2CO_3, DMAc, 120 °C	2	97	[47]
5	Fe_3O_4/DAG/Pd	Et_3N, DMF, 110 °C	0.5	96	[48]
6	NHC-Pd(II)	Na_2CO_3, DMA, 160 °C	18	99	[49]
7	Pd(OAc)$_2$@MNP	Et_3N, DMF, 100 °C	1	97	[50]
8	Pd-isatin Schiff base-γ-Fe_2O_3	Et_3N, solvent-free, 100 °C	0.5	95	[51]
9	SiO_2@Fe_3O_4-Pd	K_2CO_3, DMF, 100 °C	8	97	[52]
10	Fe_3O_4@MCM-41@Pd(0)-P2C	K_2CO_3, PEG, 120 °C	25 min	96	this work

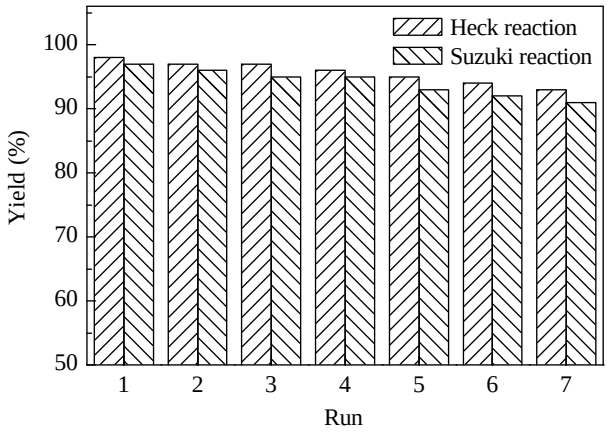

Fig. 8. Recyclability of catalyst in the Suzuki-iyaura and Heck-izoroki model reaction.

The recovery and reusability of the catalysts is of major importance in green chemistry and heterogeneous catalysis. We investigated the recovery and reusability of the Fe_3O_4@MCM-41@Pd(0)-P2C in the Suzuki-Miyaura reaction between iodobenzene (1 mmol) with phenylboronic acid (1 mmol) in PEG at 60 °C, and Heck-Mizoroki cross-coupling reaction between iodobenzene (1 mmol) and butyl acrylate (1.2 mmol) in PEG-400 at 120 °C. After completion of the reaction, as monitored by TLC, the reaction mixture was cooled to room temperature, the catalyst was easily and rapidly separated from the reaction mixture using an external magnet and washed several times with diethyl ether, then used in next run. As shown in Fig. 8, the Fe_3O_4@MCM-41@Pd(0)-P2C could be recycled over seven runs without any significant loss of its catalytic activity.

The heterogeneity of the Fe_3O_4@MCM-41@Pd(0)-P2C catalyst and the leaching of metal in the reaction mixture was examined by carrying out a hot filtration test during the Suzuki reaction between iodobenzene and phenylboronic acid. The yield of the product in half the reaction time (15 min) was 54%. The reaction was repeated and the catalyst was separated from the reaction mixture by hot filtration after 15 min. The filtrate was allowed to react further. The yield of the product under these conditions was 57%. The results from the hot filtration test indicated that no Pd leaching from the sample occurred during the catalytic reaction.

4. Conclusions

Fe_3O_4@MCM-41@Pd(0)-P2C was prepared and used as a novel, environmentally benign, and heterogeneous nanocatalyst and fully characterized using FT-IR, VSM, EDS, TEM, SEM, XRD, and TGA. The catalyst was successfully used for the Suzuki and Heck reactions under mild experimental conditions. The advantages of this system include the simple experimental procedure, utilization of an inexpensive and readily available catalyst, non-chromatographic purification of the products, simple recrystallization from diethyl ether, and avoiding the use of organic solvents, which is in agreement with green chemistry principles. In addition, this catalyst was easily separated from the reaction mixture by an external magnet and reused seven times without any significant loss of stability and activity.

Acknowledgment

The authors gratefully acknowledge Ilam University Research Council for partial financial support of this study.

References

[1] S. Rostamizadeh, M. Nojavan, R. Aryan, E. Isapoor, M. Azad, *J. Mol. Catal. A*, **2013**, 374, 102–110.
[2] M. Nikoorazm, A. Ghorbani-Choghamarani, H. Mahdavi, S. M. Esmaeili, *Microporous Mesoporous Mater.*, **2015**, 211, 174–181.
[3] S. V. Kolotilov, O. Shvets, O. Cador, N. Kasian, V. G. Pavlov, L. Ouahab, V. G. Ilyin, V. V. Pavlishchuk, *J. Solid State Chem.*, **2006**, 179, 2426–2432.
[4] M. Hasanzadeh, N. Shadjou, E. Omidinia, *Colloids Surf. B*, **2013**, 108, 52–59.
[5] M. Nikoorazm, A. Ghorbani-Choghamarani, F. Ghorbani, H. Mahdavi, Z. Karamshahi, *J. Porous Mater.*, **2015**, 22, 261–267.
[6] F. B. Zanardi, I. A. Barbosa, P. C. de Sousa Filho, L. D. Zanatta, D. L. da Silva, O. A. Serra, Y. Iamamoto, *Microporous Mesoporous Mater.*, **2016**, 219, 161–171.
[7] A. Jabbari, H. Mahdavi, M. Nikoorazm, A. Ghorbani-Choghamarani, *Res. Chem. Intermed.*, **2015**, 41, 5649–5663.
[8] N. Noori, M. Nikoorazm, A. Ghorbani-Choghamarani, *J. Porous. Mater.*, **2016**, 23, 1467–1481.
[9] M. Nikoorazm, A. Ghorbani-Choghamaran, N. Noori, *J. Porous Mater.*, **2015**, 22, 877–885.

Graphical Abstract

Chin. J. Catal., 2017, 38: 1413–1422 doi: 10.1016/S1872-2067(17)62865-1

Synthesis and characterization of a Pd(0) Schiff base complex anchored on magnetic nanoporous MCM-41 as a novel and recyclable catalyst for the Suzuki and Heck reactions under green conditions

Mohsen Nikoorazm *, Farshid Ghorbani,
Arash Ghorbani-Choghamarani, Zahra Erfani
Ilam University, Iran; University of Kurdistan, Iran

A Pd(0) Schiff base complex anchored to magnetic nanoporous MCM-41 was prepared and applied for the one-pot synthesis of Suzuki and Heck reactions in PEG to provide the target products in excellent yields.

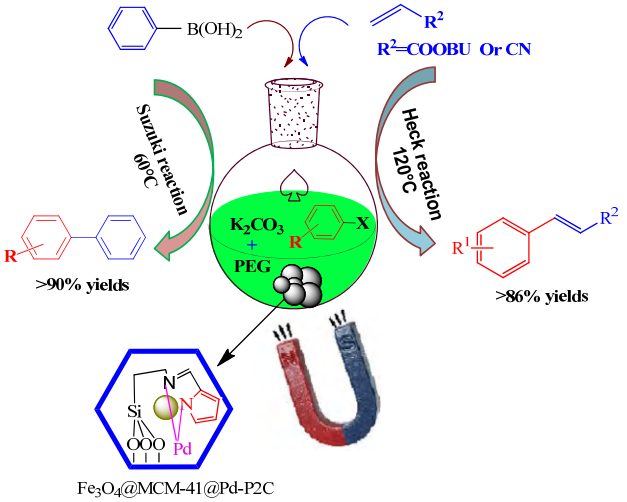

[10] M. Abdollahi-Alibeik, A. Rezaeipoor-Anari, *J. Magn. Magn. Mater.*, **2016**, 398, 205–214.
[11] S. Rostamizadeh, N. Zekri, *Res. Chem. Intermed.*, **2016**, 42, 2329–2341.
[12] M. Arruebo, W. Y. Ho, K. F. Lam, X. Q. Chen, J. Arbiol, J. Santamaria, K. L. Yeung, *Chem. Mater.*, **2008**, 20, 486–493.
[13] Z. Abbasi, S. Rezayati, M. Bagheri, R. Hajinasiri, *Chin. Chem. Lett.*, **2017**, 28, 75–82.
[14] A. Ghorbani-Choghamarani, G. Azadi, *RSC Adv.*, **2015**, 5, 9752–9758.
[15] A. Ghorbani-Choghamarani, M. Norouzi, *J. Mol. Catal. A*, **2014**, 395, 172–179.
[16] M. Hasanzadeh, M. H. Pournaghi-Azar, N. Shadjou, A. Jouyban, *RSC Adv.*, **2014**, 4, 4710–4717.
[17] A. Ghorbani-Choghamarani, B. Tahmasbi, P. Moradi, *RSC Adv.*, **2016**, 6, 43205–43216.
[18] H. P. Fan, Z. L. Qi, D. J. Sui, F. Mao, R. Z. Chen, J. Huang, *Chin. J. Catal.*, **2017**, 38, 589–596.
[19] B. Luo, J. Q. Wang, D. H. Ge, X. M. Li, X. Q. Cao, Y. Pan, H. W. Gu, *Sci. China Chem.*, **2014**, 57, 1310–1314.
[20] A. Ghorbani-Choghamarani, B. Tahmasbi, P. Moradi, *Appl. Organomet. Chem.*, **2016**, 30, 422–430.
[21] Q. Sun, L. F. Zhu, Z. H. Sun, X. J. Meng, F. S. Xiao, *Sci. China Chem.*, **2012**, 55, 2095–2103.
[22] L. Zhou, W. D. Zhang, H. F. Jiang, *Sci. China Chem.*, **2008**, 51, 241–257.
[23] H. Chen, P. Zhang, W. H. Tan, F. Jiang, R. Tang, *RSC Adv.*, **2014**, 4, 38743–38749.
[24] M. Nikoorazm, A. Ghorbani-Choghamarani, N. Noori. *Res. Chem. Intermed.*, **2016**, 42, 4621–4640.
[25] A. Ghorbani-Choghamarani, Z. Darvishnejad, B. Tahmasbi, *Inorg. Chim. Acta.*, **2015**, 435, 223–231.
[26] F. B. Zanardi, I. A. Barbosa, P. C. de Sousa Filho, L. D. Eabatta, D. L. dasilva, O. A. Serra, *Microporous Mesoporous Mater.*, **2016**, 219, 161–171.
[27] S. Rostamizadeh, M. Nojavan, R. Aryan, M. Azad, *Catal. Lett.*, **2014**, 144, 1772–1783.
[28] A. Ghorbani-Choghamarani, H. Rabiei, *Tetrahedron Lett.*, **2016**, 57, 159–162.
[29] Y. Y. Peng, J. B. Liu, X. L. Lei, Z. L. Yin, *Green Chem.*, **2010**, 12, 1072–1075
[30] M. Samarasimharseddy, G. Prabhu, T. M. Vishwanatha, V. V. Sureshbabu, *Synthesis*, **2013**, 45, 1201–1206.
[31] N. S. C. Ramesh Kumar, I. Victor Paul Raj, A. Sudalai, *J. Mol. Catal. A*, **2007**, 269, 218–224.
[32] Q. Xu, W. L. Duan, Z. Y. Lei, Z. B. Zhu, M. Shi, *Tetrahedron*, **2005**, 61, 11225–11229.
[33] N. Iranpoor, H. Firouzabadi, A. Tarassoli, M. Fereidoonnezhad, *Tetrahedron*, **2010**, 66, 2415–2421.
[34] A. Naghipour, A. Fakhri, *Catal. Commun.*, **2016**, 73, 39–45.
[35] Y. T. Leng, F. Yang, K. Wei, Y. J. Wu, *Tetrahedron*, **2010**, 66, 1244–1248.
[36] L. Wang, H. J. Li, P. H. Li, *Tetrahedron*, **2009**, 65, 364–368.
[37] S. Sobhani, Z. M. Falatooni, S. Asadi, M. Honarmand, *Catal. Lett.*, **2016**, 146, 255–268.
[38] S. Sobhani, M. S. Ghasemzadeh, M. Honarmand, F. Zarifi, *RSC Adv.*, **2014**, 83, 44166–44174.
[39] M. Nikoorazm, A. Ghorbani-Choghamarani, A. Jabbari, *J. Porous Mater.*, **2016**, 23, 967–975.
[40] S. Singha, M. Sahoo, K. M. Parida, *Dalton Trans.*, **2011**, 40, 7130–7132.
[41] M. Z. Cai , Q. H. Xu, Y. X. Huang, *J. Mol. Catal. A*, **2007**, 271, 93–97.
[42] S. Sobhani, Z. Zeraatkar, F. Zarifi, *New. J. Chem.*, **2015**, 39, 7076–7085.
[43] Y. Q. Zhang, X. W. Wei, R. Yu, *Catal. Lett.*, **2010**, 135, 256–262.
[44] M. Nasrollahzadeh, S. M. Sajadi, M. Maham, *J. Mol. Catal. A*, **2015**, 396, 297–303.
[45] Q. Xu, W. L. Duan, Z. Y. Lei, Z. B. Zhu, M. Shi, *Tetrahedron*, **2005**, 61, 11225–11229.
[46] M. Esmaeilpour, J. Javidi, *J. Chin. Chem. Soc.*, **2015**, 62, 614–626.
[47] D. S. Gaikwad, Y. K. Park, D. M. Pore, *Tetrahedron Lett.*, **2012**, 53, 3077–3081.
[48] F. W. Zhang, J. R. Niu, H. B. Wang, H. L. Yang, J. Jin, N. Liu, Y. B. Zhang, R. Li, J. T. Ma, *Mater. Res. Bull.*, **2012**, 47, 504–507.
[49] A. E. Wang, J. H. Xie, L. X. Wang, Q. L. Zhou, *Tetrahedron*, **2005**, 61, 259–266.
[50] H. Veisi, A. Sedrpoushan, S. Hemmati, *Appl. Organomet. Chem.*, **2015**, 12, 825–828.
[51] T. Chen, J. Gao, M. Shia, *Tetrahedron*, **2006**, 62, 6289–6294.
[52] Q. Zhang, X. Zhao, H. X. Wei, J. H. Li, J. Luo, *Appl. Organomet. Chem.*,

2016, doi: 10.1002/aoc.3608.
[53] S. Sobhani, F. Zarifi, *Chin. J. Catal.*, 2015, **36**, 555–563.
[54] P. H. Li, L. Wang, L. Zhang, G. W. Wang, *Adv. Synth. Catal.*, **2012**, 354, 1307–1318.

可重复使用的新型催化剂的合成、表征及在绿色条件下催化Suzuki和Heck反应: 锚合在磁性纳米多孔的MCM-41上Pd(0)希夫碱络合物

Mohsen Nikoorazm [a,*], Farshid Ghorbani [b], Arash Ghorbani-Choghamarani [a], Zahra Erfani [a]
[a]伊拉姆大学科学学院化学系, 伊拉姆, 伊朗
[b]库尔德斯坦大学自然资源学院环境系, 萨南达杰66177-15177, 伊朗

摘要: 将Pd希夫碱络合物固定在磁性的MCM-41表面上, 做为环境友好且可循环使用的新型多相纳米催化剂, 并采用红外光谱、振动探针式磁强计、能量散射谱、透射电镜、扫描电镜、热重、电感耦合等离子体发射光谱和X-射线衍射等对其进行了全面的表征. 然后将该催化剂用于以PEG为绿色溶剂的一步法Suzuki和Heck合成反应中, 均以较高收率得到目标产物. 该法主要优点为反应时间短、反应条件绿色友好、操作简便、无需使用有毒的有机溶剂、催化剂使用量低, 且底物适用性广. 更为重要的是, 通过外部磁场即可方便地将催化剂从反应混合物中分离出来, 可重复使用数次而活性和稳定性未见明显下降.

关键词: MCM-41; 磁性纳米颗粒; Suzuki反应; Heck反应; 聚乙二醇; 钯

收稿日期: 2017-04-07. 接受日期: 2017-05-16. 出版日期: 2017-08-05.
*通讯联系人. 电话/传真: +98-843-2227022; 电子信箱: e_nikoorazm@yahoo.com
本文的英文电子版由Elsevier出版社在ScienceDirect上出版(http://www.sciencedirect.com/science/journal/18722067).